



HAL
open science

α -As₂Te₃ as a platform for the exploration of the electronic band structure of single layer β -tellurene

Lama Khalil, Pietro Maria Forcella, Geoffroy Kremer, Federico Bisti, Julien Chaste, Jean-Christophe Girard, Fabrice Oehler, Marco Pala, Jean-Francois Dayen, Demetrio Logoteta, et al.

► To cite this version:

Lama Khalil, Pietro Maria Forcella, Geoffroy Kremer, Federico Bisti, Julien Chaste, et al.. α -As₂Te₃ as a platform for the exploration of the electronic band structure of single layer β -tellurene. Physical Review B, 2022, 106 (12), pp.125152. 10.1103/physrevb.106.125152 . hal-03865011

HAL Id: hal-03865011

<https://hal.science/hal-03865011>

Submitted on 22 Nov 2022

HAL is a multi-disciplinary open access archive for the deposit and dissemination of scientific research documents, whether they are published or not. The documents may come from teaching and research institutions in France or abroad, or from public or private research centers.

L'archive ouverte pluridisciplinaire **HAL**, est destinée au dépôt et à la diffusion de documents scientifiques de niveau recherche, publiés ou non, émanant des établissements d'enseignement et de recherche français ou étrangers, des laboratoires publics ou privés.



Distributed under a Creative Commons Attribution 4.0 International License

α -As₂Te₃ as a platform for the exploration of the electronic band structure of single layer β -tellurene

Lama Khalil,¹ Pietro Maria Forcella,² Geoffroy Kremer^{1,*}, Federico Bisti,² Julien Chaste,¹ Jean-Christophe Girard,¹ Fabrice Oehler,¹ Marco Pala,¹ Jean-Francois Dayen,^{3,4} Demetrio Logoteta,¹ Mark Goerbig,⁵ François Bertran,⁶ Patrick Le Fèvre,⁶ Emmanuel Lhuillier,⁷ Julien Rault,⁶ Debora Pierucci,⁶ Gianni Profeta,^{2,8} and Abdelkarim Ouerghi^{1,†}

¹Université Paris-Saclay, CNRS, Centre de Nanosciences et de Nanotechnologies, 91120, Palaiseau, France

²Dipartimento di Scienze Fisiche e Chimiche, Università dell'Aquila, Via Vetoio, 67100 L'Aquila, Italy

³Université de Strasbourg, IPCMS-CMRS UMR 7504, 23 Rue du Loess, 67034 Strasbourg, France

⁴Institut Universitaire de France, 1 rue Descartes, 75231 Paris cedex 05, France

⁵Laboratoire de Physique des Solides, Université Paris-Saclay, CNRS UMR 8502, 91405 Orsay Cedex, France

⁶Synchrotron SOLEIL, L'Orme des Merisiers, Départementale 128, F-91190 Saint-Aubin, France

⁷Sorbonne Université, CNRS, Institut des NanoSciences de Paris, INSP, F-75005 Paris, France

⁸CNR-SPIN L'Aquila, Via Vetoio 10, I-67100 L'Aquila, Italy



(Received 12 July 2022; accepted 12 September 2022; published 30 September 2022)

Arsenic telluride, As₂Te₃, is a layered van der Waals (vdW) semiconducting material usually known for its thermoelectric properties. It is composed of layers stacked together via weak vdW interactions, which can consequently be exfoliated into thin two-dimensional layers. Here, we studied the electronic properties of the α phase of As₂Te₃ by using angle-resolved photoemission spectroscopy (ARPES) and density-functional theory (DFT). In addition to the spectroscopic signature of α -As₂Te₃, we were able to isolate anisotropic 2D electronic states, decoupled from the α -As₂Te₃ electronic structure, that we propose to ascribe to single layer (SL) β -tellurene. Our findings are supported by theoretical investigations using DFT, which reproduce the main ARPES experimental features. Our work thereby proposes α -As₂Te₃ (100) surface as an interesting platform for the experimental exploration of the electronic band structure of SL β -tellurene, which has been difficult to experimentally access otherwise.

DOI: [10.1103/PhysRevB.106.125152](https://doi.org/10.1103/PhysRevB.106.125152)

I. INTRODUCTION

Quas layered A₂X₃-type chalcogenides (A = As, Sb, Bi; X = S, Se, Te), are generally narrow band-gap semiconductors which have attracted interest due to their interesting electronic and thermal properties [1–3]. They all share a lamellar crystal structure, held by weak van der Waals (vdW) interlayer forces in one direction, but most of them crystallize in several polymorphs depending on the activity of the cation lone electron pair [4]. For example, arsenic telluride is a polymorphic compound known to exhibit at least two phases: α -As₂Te₃ (monoclinic) and β -As₂Te₃ (rhombohedral), originating from distinct stacking sequences. The monoclinic α phase of As₂Te₃ is the most common, as it is the most stable at room temperature and crystallizes in a monoclinic structure, with the lattice parameters $a = 14.345$ Å, $b = 4.016$ Å, $c = 9.891$ Å, and $\beta = 95.06^\circ$, as previously reported by Carron *et al.* [5]. The crystal structure of the α -As₂Te₃ [Fig. 1(a)] is composed of covalent layers with a zigzag profile, stacked along the a axis by vdW interaction, which provide straightforward cleavage plane parallel to b - and c axes. Several preceding investigations have focused on

the phase transition from α -As₂Te₃ to other crystalline form [2,6–11], but the electronic band structure of the α phase has not yet been determined experimentally. In addition, the particular crystal structure of the (100) surface α -As₂Te₃ could also host and stabilize specific bidimensional species from the tellurene or arsenene types [12,13], whose electronic properties have been little explored so far. Particularly, β -tellurene is an interesting material because it is a semiconducting monolayer that combines air stability, high room-temperature mobility [14], and low thermal conductivity [15]. These properties make it an excellent candidate for both electronic and thermoelectric applications. The use of (100) α -As₂Te₃ as a platform to explore the fundamental properties of this type of compound, via the creation of As or Te defects, has not yet been explored experimentally.

In the present work, we directly explore the electronic band structure of α -As₂Te₃ by using angle-resolved photoemission spectroscopy (ARPES). We observe clear spectroscopic signatures of the bulk contributions of α -As₂Te₃ in the (100) plane after crystal cleavage in agreement with our low-energy electron diffraction (LEED) measurements. We further highlight the presence of additional two-dimensional (2D) and anisotropic electronic states which cannot be assigned to any α -As₂Te₃ (100) surface states or any known reconstructions. The features of these extra electronic states are very specific, and we could only match them to the electronic states from

*geoffroy.kremer@univ-lorraine.fr

†abdelkarim.ouerghi@c2n.upsaclay.fr

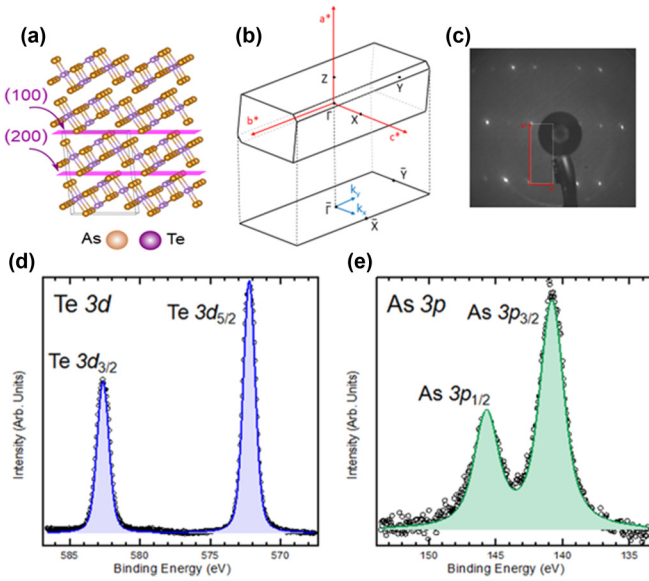


FIG. 1. (a) Crystal structure of α -As₂Te₃. Arsenic and tellurium atoms are represented in purple and orange spheres, respectively. (b) Schematic diagram of the bulk 3D BZ of α -As₂Te₃ and the 2D BZ of the projected (100) surface. (c) LEED pattern at 113 eV showing the diffraction spots due to the (100) surface plane of α -As₂Te₃ and the reciprocal lattice vectors \mathbf{b}^* and \mathbf{c}^* in red. (d), (e) High-resolution XPS spectra of Te 3d and As 3p core levels measured at $h\nu = 800$ eV. Experimental points are displayed in circles; the blue and green solid lines represent the envelope of the fitted components.

β -tellurene single layer (SL). In particular, we observe a well-defined band dispersing at the center of the Brillouin zone (BZ) and localized just below the Fermi level (E_F), which are reproduced by density-functional theory (DFT) calculations on β -tellurene. Complementary scanning tunneling microscopy (STM) measurements show defect areas that support the existence of an additional compound domains on pure α -As₂Te₃.

II. RESULTS

The polymorph structure of As₂Te₃ can affect its electronic and physical properties; consequently, the precise determination of the material phase structure is crucial for subsequent ARPES investigations. To determine the crystal structure of our As₂Te₃ samples, we conducted a comprehensive characterization by employing complementary techniques. In particular, x-ray diffraction (XRD) (see Supplemental Material [16], Fig. S1), LEED measurement [Fig. 1(c)] and x-ray photoemission spectroscopy (XPS) analysis [Figs. 1(d) and 1(e)] confirm that our specimens correspond to α -As₂Te₃ with lattice parameters $a = 14.345$ Å, $b = 4.016$ Å, $c = 9.891$ Å, and $\beta = 95.06^\circ$, consistent with the values previously reported by Carron *et al.* [5]. Figure 1(c) shows the LEED pattern of the cleaved α -As₂Te₃ surface. The diffraction pattern forms a regular rectangular lattice (marked as red vectors), the aspect ratio of which is $R = 2.50 \pm 0.03$, as measured directly on the LEED image. Using the real-space lattice parameters previously determined by XRD, we obtained the following reciprocal lengths: $\mathbf{b}^* = 2\pi/b = 1.564$ Å⁻¹ and

$\mathbf{c}^* = 2\pi/(c \sin \beta) = 0.6379$ Å⁻¹. As the vectors \mathbf{b}^* and \mathbf{c}^* are perpendicular in the reciprocal space, the theoretical diffraction pattern of the (100) surface should appear as a rectangular lattice of aspect ratio $R_{\text{theoretical}} = 2.45$ for any close orientation. In the limit of the LEED angular alignment, the observed aspect ratio $R = 2.50$ and the clear rectangular shape of the LEED pattern confirm that the cleaved surface corresponds to the (100) α -As₂Te₃ surface. All the photoemission data were extracted from this cleaved surface. This orientation is also confirmed by our recent STM study (see Ref. [3]). However, the cleavage plane is not fully smooth and the ARPES intensity map (see Fig. S2) shows that flat domain extends up to 300×300 μm approximately. All the ARPES and photoemission data were extracted from this cleaved surface. The ARPES experiments were repeated on three different As₂Te₃ crystals, all obtained commercially from HQ Graphene (see Fig. S3).

In Figs. 1(d) and 1(e), we show the XPS spectra for the Te 3d and As 3p core levels acquired at $h\nu = 800$ eV. After the subtraction of a Shirley background, the spectra were fitted using Voigt functions. The Te 3d spectrum presents two peaks at 572.2 and 582.6 eV binding energy (BE), which are attributed to the Te 3d_{5/2} and Te 3d_{3/2} levels. Similarly, two peaks are also visible for the As 3p core level, corresponding to the As 3p_{3/2} (BE = 140.8 eV) and As 3p_{1/2} (BE = 145.7 eV) contributions. No additional components at higher BEs are visible in each of the spectra, meaning that our (100) α -As₂Te₃ surface is free of external contaminant, notably oxygen [17–19].

We now explore the electronic band structure of α -As₂Te₃ measured by ARPES using a series of photon energies ranging from $h\nu = 19$ eV to $h\nu = 68$ eV along the $\bar{\Gamma} - \bar{X}$ high-symmetry direction of the BZ, as depicted in Fig. 2. The ARPES signal at energies below 0.2 eV from E_F is characterized by a complex interplay of dispersive bands changing in position and intensity with the probing photon energy. Remarkably, a sharp band disperses at the $\bar{\Gamma}$ point of the BZ with a Λ shape, as evidenced by the zoom (bottom panels) on the first hundreds of meV below E_F . The shape and dispersion of this sharp band, which we name SS in the following, does not seem to be affected by any modification on the probing photon energy as more precisely shown in a series of photon-energy dependent ARPES measurements illustrated in Fig. S4. We consequently conclude that this state has a pure 2D character. The 3D dispersion of the bands at higher BEs is more difficult to be precisely accessed since the bands are all mixed together.

As shown in Figs. 3(a)–3(d), we also performed constant-energy surface measurements at $h\nu = 27$ eV. The isoenergy map at E_F presents a single point at the center of the BZ [Fig. 3(a)], which evolves into a circular shape at 100 meV below E_F [Fig. 3(b)], suggesting at first glance an isotropic character of SS. Nevertheless, as observed in Figs. 3(c) and 3(d), this feature exhibits a rectangular shape at higher BEs, namely at 200 and 300 meV BEs, around the $\bar{\Gamma}$ point, indicating that the constant-energy surface is anisotropic. This is further confirmed by the ARPES spectra obtained along the $\bar{\Gamma} - \bar{X}$ (green), $\bar{\Gamma} - \bar{Y}$ (blue), and intermediate (red) high-symmetry lines, showing different effective masses of SS along each of these directions [see Figs. 3(e)–3(g) and

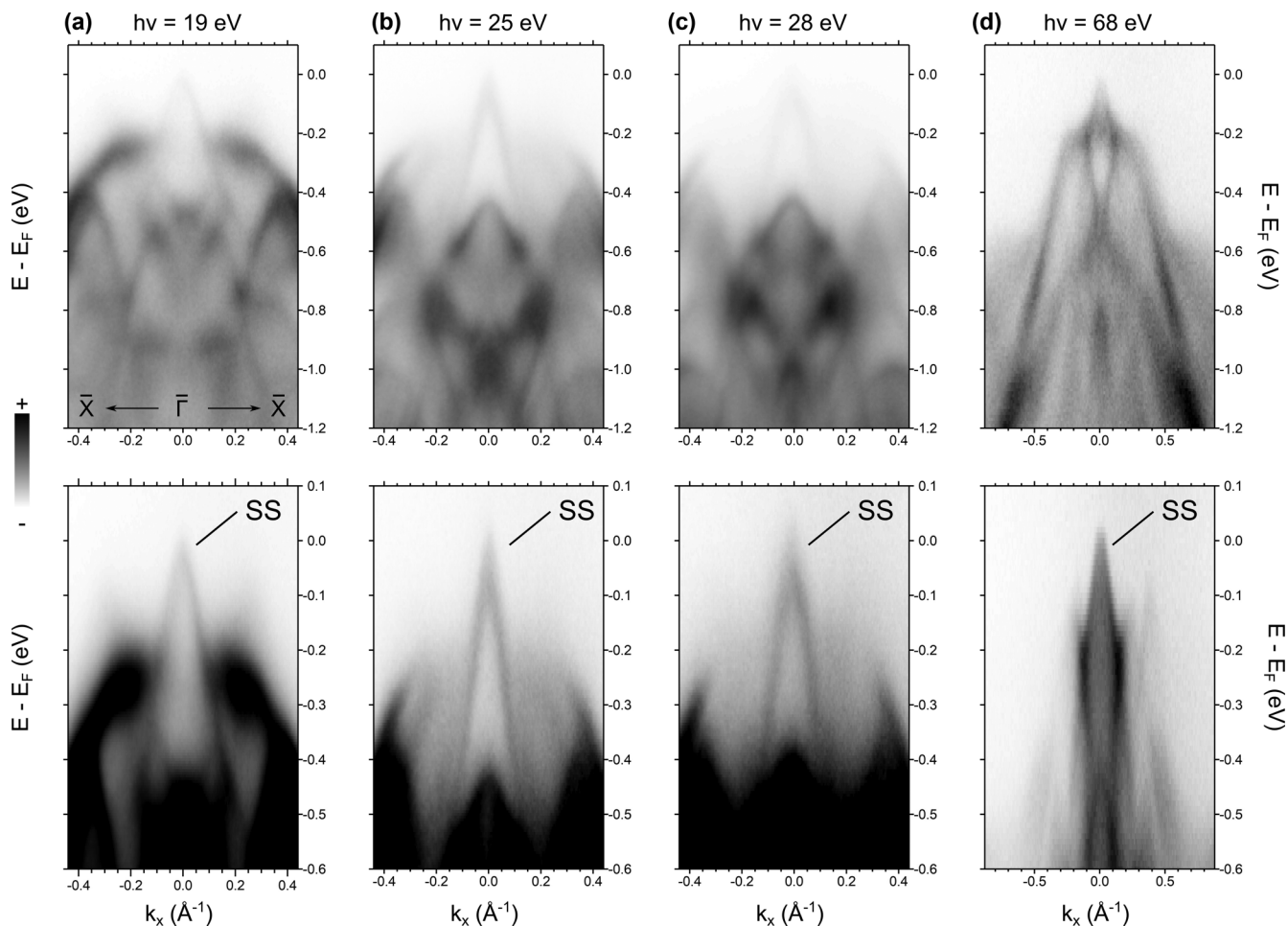


FIG. 2. ARPES spectra ($T = 50$ K) of α -As₂Te₃ measured along the $\bar{X}-\bar{\Gamma}-\bar{X}$ high symmetry direction of the 2D Brillouin zone on a large scale (top) and zoomed in (bottom) for (a) $h\nu = 19$ eV, (b) $h\nu = 25$ eV, (c) $h\nu = 28$ eV, and (d) $h\nu = 68$ eV.

Fig. S5)]. This unambiguously confirms that SS has an anisotropic character. The same SS states were observed on two other cleaved As₂Te₃ samples (see Fig. S3).

In order to get more insights into the electronic band structure of α -As₂Te₃, we performed bulk projected band-structure calculations [blue-green-yellow colored lines in

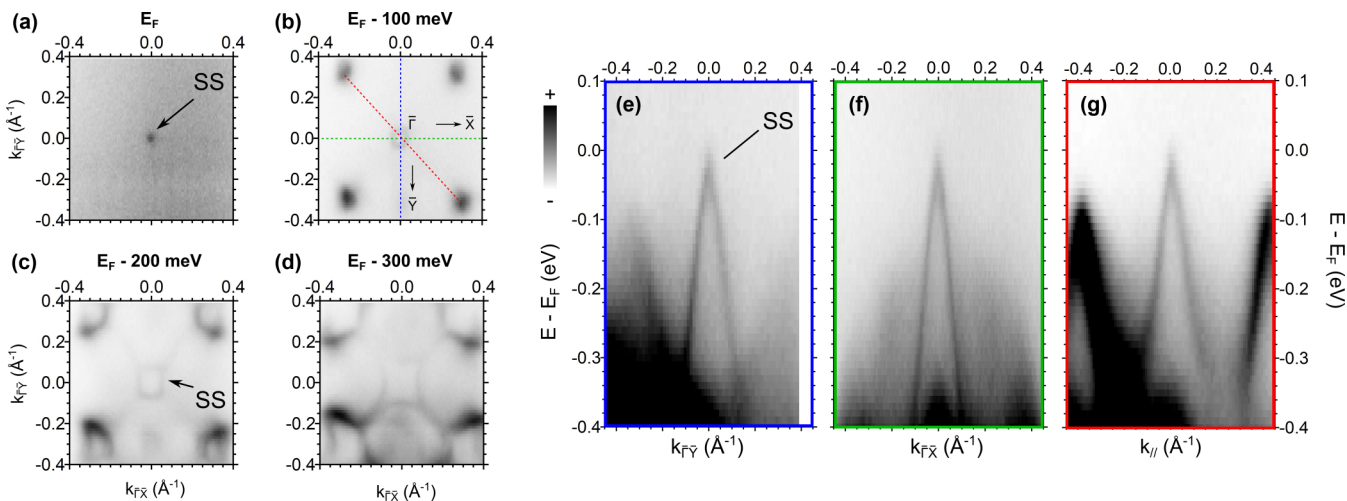


FIG. 3. ARPES constant-energy surfaces of α -As₂Te₃ ($T = 50$ K and $h\nu = 27$ eV) for (a) E_F ; (b) E_F-100 meV; (c) E_F-200 meV; and (d) E_F-300 meV. (e)–(g) Corresponding ARPES spectra along selected directions in the 2D BZ, as schematized by colored dashed lines in panel (b).

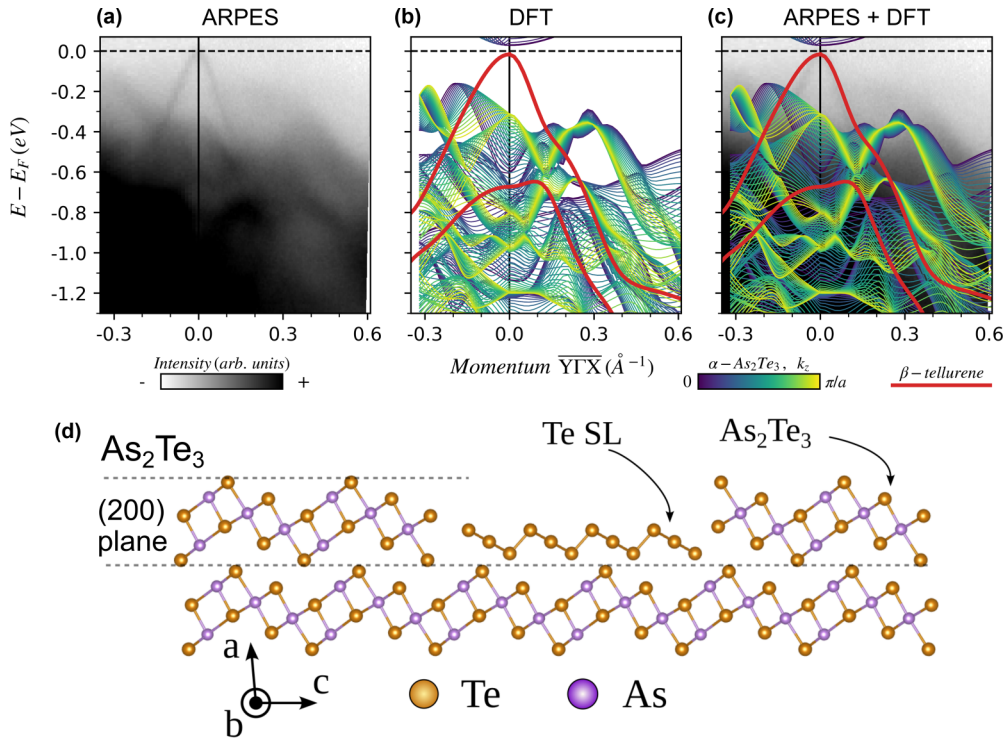


FIG. 4. (a) ARPES spectrum (square-root color scale) of α - As_2Te_3 measured along the $\bar{Y}-\bar{\Gamma}-\bar{X}$ high-symmetry direction ($T = 50$ K and $h\nu = 27$ eV) compared with (b) theoretical electronic band structure of SL β -tellurene (red curve) on top of bulk α - As_2Te_3 band structure (blue-green-yellow colored lines depending on the k_z vector). (c) Comparison between ARPES spectrum and calculations. (d) Structural model for α - As_2Te_3 (100) surface with SL β -tellurene formation that we propose to be measured with ARPES experiments (not the model we used for DFT calculations).

Figs. 4(b) and 4(c)], i.e., an overlap of the bulk band structure for different values of k_z along the out-of-plane $\Gamma-Z$ direction in the 3D BZ of the crystal [see Fig. 1(b)]. Indeed, some integrations along the k_z direction can occur in ARPES for quasi-2D materials [20–22]. As shown in Figs. 4(a)–4(c), we directly compare these calculations with the ARPES spectrum obtained at $h\nu = 27$ eV along the $\bar{Y}-\bar{\Gamma}-\bar{X}$ high-symmetry direction, which both resolve the SS state near E_F (further discussed in the following paragraph) and the other bands at higher BEs. From this comparison, we remark that most of the experimentally measured features at BEs higher than 0.2 eV are well reproduced by the calculations, confirming the 3D character of most states in this energy region. Nevertheless, some of the experimentally observed bands in this high-BE region are not reproduced by the DFT simulations. This observation is quite obvious from 0.2 eV BE to E_F , as the 2D anisotropic SS is completely absent of the projected 3D α - As_2Te_3 band structure. This discrepancy also remains in the case of DFT calculations performed on α - As_2Te_3 (100) surface alone, i.e., by considering a three-layer slab along the (100) surface and not only the bulk structure (see Fig. S6). Consequently, we can fully rule out As_2Te_3 bulk or surface states as the origin of the anisotropic 2D electronic state SS.

In addition, we discarded also its origin coming from surface defects since, from our theoretical calculations (see Supplemental Material), no atomic vacancy seems to develop conical electronic states around the $\bar{\Gamma}$ point (see Fig. S7). After having theoretically explored other possibilities, also including the formation of an α -arsenene single layer (see

Supplemental Material and Fig. S8), we found an interesting electronic structure for a SL β -tellurene.

As SL β -tellurene or arsenene could form from α - As_2Te_3 by creating As or Te defects [see Fig. 4(d) and Fig. S9)], we have theoretically investigated the superposition of the electronic structure of bulk α - As_2Te_3 [blue-green-yellow colored lines, Figs. 4(b) and 4(c)] with the one of a the SL β -tellurene [red lines in Figs. 4(b) and 4(c)] and SL arsenene (Fig. S8) band structures. While the simulated SL arsenene band structure fails to match the experiment, the one of SL β -tellurene reproduces well the band dispersion of SS around $\bar{\Gamma}$. Furthermore, we can also identify at least one additional state associated with β -tellurene which is mixed with those of α - As_2Te_3 at higher BEs, explaining the complicated band structure in this energy range. A one-to-one comparison between ARPES and SL β -tellurene DFT calculation is given in Fig. 4(c) and shows a good correspondence. In addition to its position in energy and reciprocal space, the SL β -tellurene DFT also reproduces the anisotropic character of the SS band, due to the anisotropic crystal structure of β -tellurene (in the direct space). Indeed, in the same fashion as black phosphorus [23] or its SL counterpart, phosphorene [24], β -tellurene exhibits a strong anisotropic structure with armchair and zigzag directions rotated by 90° [25]. This hypothesis is in good correspondence with the STM measurements we performed in Fig. S10 and Fig. S11. In particular, our STM images exhibit black stripes over a long range which could be related to SL tellurene ribbons contributing to the ARPES spectral weight. Indeed, the difference of height between these black

stripes and the α -As₂Te₃ terraces equals 8 pm, which cannot correspond to the height of an α -As₂Te₃ double- (\sim 14Å) or single (\sim 7Å) step. In Fig. 4(d), we propose a picture for the formation of SL β -tellurene domain replacing α -As₂Te₃ plane and creating the area we observe with ARPES, and consequently explaining the SS band.

III. METHODS

A. Photoemission spectroscopy

ARPES experiments were performed at the CASSIOPEE beamline of the SOLEIL Synchrotron light source. The CASSIOPEE beamline is equipped with a Scienta R4000 hemispherical electron analyzer whose angular acceptance is $\pm 15^\circ$ (Scienta Wide Angle Lens). High-quality samples from the HQ Graphene Co. were cleaved in UHV at a base pressure better than 1×10^{-10} mbar. The experiment was performed at $T = 50$ K. The total angle and energy resolutions were 0.25° and 16 meV, respectively. The incident photon beam was focused into a $50\text{-}\mu\text{m}$ spot (in diameter) on the sample surface. All ARPES measurements were performed with a linear horizontal polarization.

B. Scanning tunneling microscopy

STM experiments are performed at $T = 77$ K using an LT-STM (Scienta-Omicron). The sample has been prepared in the same conditions compared to ARPES measurements, cleaved at a base pressure better than 1×10^{-10} mbar and transferred immediately in the precooled STM head. STM images are acquired in the constant current mode.

C. Theoretical calculations

The Vienna *Abinitio* Simulation Package (VASP) [26,27] with Perdew-Burke-Ernzerhof generalized gradient approximation exchange-correlation energy functional is employed in our first-principles calculations [28]. Integration over the Brillouin zone was performed using a Gaussian smearing for the partial occupancies with a 0.2 eV width. The plane-wave cut-off energy was 600 eV and spin-orbit coupling (SOC) was taken into account in all calculations. For the bulk α -As₂Te₃,

the k-point sampling grid was $4 \times 14 \times 6$. Tellurene was described with $20 \times 20 \times 1$ k-point grid in the β phase with optimized lattice constants of $a = 4.18$ Å and $b = 5.80$ Å, in agreement within a few percent as reported in Ref. [29] and references therein.

IV. CONCLUSIONS

To conclude, from a fundamental ARPES investigation of the electronic band structure of α -As₂Te₃, we unexpectedly detect, in addition to the bulk As₂Te₃ electronic band structure, a surface-state signal which nicely resembles the expected one from SL β -tellurene. STM measurements indeed confirm the presence of domains of another compound on the pure α -As₂Te₃(001) surface, and we suggest a feasible mechanism of β -tellurene formation by As removal. This scenario is strongly supported by advanced *abinitio* calculations, which in particular rule out the possibility to explain this electronic surface state by the existence of surface defects or pure surface state of As₂Te₃. The present study opens the way for future precise exploration of the momentum-resolved unoccupied part of the band structure, in particular the conduction band, which is predicted to be separated from the valence band by a direct electronic band gap of 1.47 eV [12] at the center of the BZ. This could be of high interest for time-resolved ARPES investigations with infrared pulses, in particular in the perspective of the exploration of excitonic behaviors [30–32].

The datasets generated during and/or analyzed during the current study are available from the corresponding author on reasonable request [33].

ACKNOWLEDGMENTS

We acknowledge the financial support by MagicValley (Grant No. ANR-18-CE24-0007) and Graskop (Grant No. ANR-19-CE09-0026). P.M.F. wishes to acknowledge financial support from the Erasmus Plus for Traineeship from the University of L'Aquila. G.P. acknowledges the Italian Ministry for Research and Education through PRIN-2017 project "Tuning and understanding Quantum phases in 2D materials Quantum 2D" (IT-MIUR Grant No. 2017Z8TS5B).

The authors declare no competing interests.

-
- [1] Y. Sharma and P. Srivastava, First principles investigation of electronic, optical and transport properties of α - and β -phase of arsenic telluride, *Opt. Mater. (Amst.)* **33**, 899 (2011).
- [2] C. Morin, S. Corallini, J. Carreaud, J-B. Vaney, G. Delaizir, J-C. Crivello, E. B. Lopes, A. Piarristeguy, J. Monnier, C. Candolfi *et al.*, Polymorphism in thermoelectric As₂Te₃, *Inorg. Chem.* **54**, 9936 (2015).
- [3] L. Khalil, J-C. Girard, D. Pierucci, F. Bisti, J. Chaste, F. Oehler, C. Gréboval, U. N. Noubé, J-F. Dayen, D. Logoteta *et al.*, Electronic band gap of van der Waals α -As₂Te₃ crystals, *Appl. Phys. Lett.* **119**, 043103 (2020).
- [4] J. A. Sans, F. J. Manjón, A. L. de Jesus Pereira, J. Ruiz-Fuertes, C. Popescu, A. Muñoz, P. Rodríguez-Hernández, J. Pellicer-Porres, V. P. Cuenca-Gotor, J. Contreras-García *et al.*, Unveiling the role of the lone electron pair in sesquioxides at high pressure: compressibility of β -Sb₂O₃, *Dalton Trans.* **50**, 5493 (2021).
- [5] G. J. Carron, The crystal structure and powder data for arsenic telluride, *Acta Crystallogr.* **16**, 338 (1963).
- [6] S. Toscani, J. Dugué, R. Ollitrault, and R. Céolin, Polymorphism of As₂Te₃: Structural studies and thermal behaviour of rhombohedral β -As₂Te₃, *Thermochim. Acta* **186**, 247 (1991).
- [7] T. J. Scheidemantel, J. F. Meng, and J. V. Badding, Thermoelectric power and phase transition of polycrystalline As₂Te₃ under pressure, *J. Phys. Chem. Solids* **66**, 1744 (2005).
- [8] J-B. Vaney, J. Carreaud, G. Delaizir, A. Pradel, A. Piarristeguy, C. Morin, E. Alleno, J. Monnier, A. P. Gonçalves, C. Candolfi *et al.*, High-Temperature thermoelectric properties

- of Sn-doped β -As₂Te₃, *Adv. Electron. Mater.* **1**, 1400008 (2015).
- [9] T. J. Scheidemantel and J. V. Badding, Electronic structure of β -As₂Te₃, *Solid State Commun.* **127**, 667 (2003).
- [10] V. Cuenca-Gotor, J. A. Sans, J. Ibanez, C. Popescu, O. Gomis, R. Vilaplana, F. J. Manjon, A. Leonardo, E. Sagasta, A. Suarez-Alcubilla *et al.*, Structural, vibrational, and electronic study of α -As₂Te₃ under compression, *J. Phys. Chem. C* **120**, 19340 (2016).
- [11] L. Dai, Y. Zhuang, H. Li, L. Wu, H. Hu, K. Liu, L. Yang, and C. Pu, Pressure-induced irreversible amorphization and metalization with a structural phase transition in arsenic telluride, *J. Mater. Chem. C* **5**, 12157 (2017).
- [12] Z. Zhu, X. Cai, S. Yi, J. Chen, Y. Dai, C. Niu, Z. Guo, M. Xie, F. Liu, J-H. Cho *et al.*, Multivalency-driven Formation of Te-based Monolayer Materials: A Combined First Principles and Experimental Study, *Phys. Rev. Lett.* **119**, 106101 (2017).
- [13] J. Shah, W. Wang, H. M. Sohail, and R. I. G. Uhrberg, Experimental evidence of monolayer arsenene: An exotic 2D semiconducting material, *2D Mater.* **7**, 025013 (2020).
- [14] Y. Wang, G. Qiu, R. Wang, S. Huang, Q. Wang, Y. Liu, Y. Du, W. A. Goddard, M. J. Kim, X. Xu *et al.*, Field-effect transistors made from solution-grown two-dimensional tellurene, *Nat. Electron.* **1**, 228 (2018).
- [15] Z. Gao, F. Tao, and J. Ren, Unusually low thermal conductivity of atomically thin 2D tellurium, *Nanoscale* **10**, 12997 (2018).
- [16] See Supplemental Material at <http://link.aps.org/supplemental/10.1103/PhysRevB.106.125152> for additional data including XRD, ARPES, and STM measurements, and DFT calculations.
- [17] A. J. Henegar and T. Gougousi, Native oxide transport and removal during the atomic layer deposition of Ta₂O₅ on InAs(100) surfaces, *J. Vac. Sci. Technol. A: Vac., Surf., Film* **34**, 031101 (2016).
- [18] M. O. Reese, C. L. Perkins, J. M. Burst, S. Farrell, T. M. Barnes, S. W. Johnston, D. Kuciauskas, T. A. Gessert, and W. K. Metzger, Intrinsic surface passivation of CdTe, *J. Appl. Phys.* **118**, 155305 (2015).
- [19] T. Gougousi and L. Ye, Interface between atomic layer deposition Ta₂O₅ films and GaAs(100) surfaces, *J. Phys. Chem. C* **116**, 8924 (2012).
- [20] D. W. Latzke, W. Zhang, A. Suslu, T.-R. Chang, H. Lin, H-T. Jeng, S. Tongay, J. Wu, A. Bansil, and A. Lanzara, Electronic structure, spin-orbit coupling, and interlayer interaction in bulk MoS₂ and WS₂, *Phys. Rev. B* **91**, 235202 (2015).
- [21] H. Henck, D. Pierucci, J. Zribi, F. Bisti, E. Papalazarou, J.-C. Girard, J. Chaste, F. Bertran, P. Le Fèvre, F. Sirotti *et al.*, Evidence of direct electronic band gap in two-dimensional van der Waals indium selenide crystals, *Phys. Rev. Mater.* **3**, 034004 (2019).
- [22] G. Kremer, M. Rumo, C. Yue, A. Pulkkinen, C. W. Nicholson, T. Jaouen, F. O. von Rohr, P. Werner, and C. Monney, Ultrafast dynamics of the surface photovoltage in potassium-doped black phosphorus, *Phys. Rev. B* **104**, 035125 (2021).
- [23] X. Mu, J. Wang, and M. Sun, Two-dimensional black phosphorus: Physical properties and applications, *Mater. Today Phys.* **8**, 92 (2019).
- [24] A. Carvalho, M. Wang, X. Zhu, A. S. Rodin, H. Su, A. Castro Neto, and H. Antonio, Phosphorene: From theory to applications, *Nat. Rev. Mater.* **1**, 16061 (2016).
- [25] Z. Shi, R. Cao, K. Khan, A. K. Tareen, X. Liu, W. Liang, Y. Zhang, C. Ma, Z. Guo, X. Luo *et al.*, Two-dimensional tellurium: Progress, challenges, and prospects, *Nano-Micro Lett.* **12**, 1 (2020).
- [26] G. Kresse and J. Furthmüller, Efficient iterative schemes for ab initio total-energy calculations using a plane-wave basis set, *Phys. Rev. B* **54**, 11169 (1996).
- [27] G. Kresse and J. Furthmüller, Efficiency of ab-initio total energy calculations for metals and semiconductors using a plane-wave basis set, *Comput. Mater. Sci.* **6**, 15 (1996).
- [28] J. P. Perdew, K. Burke, and M. Ernzerhof, Generalized Gradient Approximation Made Simple, *Phys. Rev. Lett.* **77**, 3865 (1996).
- [29] K. Wu, H. Ma, Y. Gao, W. Hu, and J. Yang, Highly-efficient heterojunction solar cells based on two-dimensional tellurene and transition metal dichalcogenides, *J. Mater. Chem. A* **7**, 7430 (2019).
- [30] A. Rustagi and A. F. Kemper, Photoemission signature of excitons, *Phys. Rev. B* **99**, 125303 (2018).
- [31] D. Christiansen, M. Selig, E. Malic, R. Ernstorfer, and A. Knorr, Theory of exciton dynamics in time resolved ARPES: Intra- and intervalley scattering in two-dimensional semiconductors, *Phys. Rev. B* **100**, 205401 (2019).
- [32] S. Dong, M. Puppini, T. Pincelli, S. Beaulieu, D. Christiansen, H. Hübener, C. W. Nicholson, R. P. Xian, M. Dendzik, Y. Deng *et al.*, Direct measurement of key exciton properties: Energy, dynamics, and spatial distribution of the wave function, *Nat. Sci.* **1**, e11010 (2021).
- [33] The datasets generated during and/or analyzed during the current study are available from the corresponding author on reasonable request.